PLOS ONE

RESEARCH ARTICLE

# Biophysical and structural characterization of a zinc-responsive repressor of the MarR superfamily

**Paloma Fernández Varela**[1,2¤]*, **Christophe Velours**[3¤], **Magali Aumont-Niçaise**[4¤], **Blandine Pineau**[1], **Pierre Legrand**[1], **Isabelle Poquet**[5]

**1** Synchrotron SOLEIL, L'Orme des Merisiers, Gif-sur-Yvette, France, **2** Laboratoire d'Enzymologie et Biochimie Structurales, CNRS Gif-sur-Yvette, France, **3** IMAGIF, CNRS Gif-sur-Yvette, France, **4** Institut de Biochimie et Biophysique Moléculaire et Cellulaire, Université Paris-Sud, Orsay, France, **5** Micalis Institute, INRA, AgroParisTech, Université Paris-Saclay, Jouy-en-Josas, France

¤ Current address: Institute for Integrative Biology of the Cell, CEA, CNRS, Université Paris-Saclay, Gif-sur-Yvette, France
* paloma.fernandez-varela@i2bc.paris-saclay.fr





**Citation:** Varela PF, Velours C, Aumont-Niçaise M, Pineau B, Legrand P, Poquet I (2019) Biophysical and structural characterization of a zinc-responsive repressor of the MarR superfamily. PLoS ONE 14 (2): e0210123. https://doi.org/10.1371/journal.pone.0210123

**Editor:** Eugene A. Permyakov, Russian Academy of Medical Sciences, RUSSIAN FEDERATION

**Received:** September 25, 2018

**Accepted:** December 17, 2018

**Published:** February 12, 2019



**Data Availability Statement:** The structure data from this publication have been deposited in the PDB database https://www.rcsb.org/ and assigned the accession number 6FI9.

**Funding:** This work was supported by the French Infrastructure for Integrated Structural Biology (FRISBI), ANR-10-INSB-05-01.

**Competing interests:** The authors have declared that no competing interests exist.

## Abstract

The uptake of zinc, which is vital in trace amounts, is tightly controlled in bacteria. For this control, bacteria of the *Streptococcaceae* group use a Zn(II)-binding repressor named ZitR in lactococci and AdcR in streptococci, while other bacteria use a Zur protein of the Ferric uptake regulator (Fur) superfamily. ZitR and AdcR proteins, characterized by a winged helix-turn-helix DNA-binding domain, belong to the multiple antibiotic resistance (MarR) superfamily, where they form a specific group of metallo-regulators. Here, one such Zn(II)-responsive repressor, ZitR of *Lactococcus lactis* subspecies *cremoris* strain MG1363, is characterized. Size Exclusion Chromatography-coupled to Multi Angle Light Scattering, Circular Dichroism and Isothermal Titration Calorimetry show that purified ZitR is a stable dimer complexed to Zn(II), which is able to bind its two palindromic operator sites on DNA fragments. The crystal structure of ZitR holo-form ($Zn(II)_4$-$ZitR_2$), has been determined at 2.8 Å resolution. ZitR is the fourth member of the MarR metallo-regulator subgroup whose structure has been determined. The folding of ZitR/AdcR metallo-proteins is highly conserved between both subspecies (*cremoris* or *lactis*) in the *Lactococcus lactis* species and between species (*Lactococcus lactis* and *Streptococcus pneumoniae or pyogenes*) in the *Streptococcaceae* group. It is also similar to the folding of other MarR members, especially in the DNA-binding domain. Our study contributes to better understand the biochemical and structural properties of metallo-regulators in the MarR superfamily.

## Introduction

Zinc is a widespread transition metal and, although Zn(II) cation is toxic at high concentrations, it is absolutely essential for life [1]. Zn(II) is necessary for many cellular functions including DNA replication, transcription, and translation. At a molecular level, it performs an

essential structural role in protein or protein domain folding (e.g. zinc-finger proteins. . .), and it is also important for many enzymatic activities, as more than 300 enzymes bind Zn(II) [2].

To maintain cytoplasmic Zn(II) homeostasis, bacterial cells have to tightly control its transport. Zn(II) ABC uptake systems, which are of high affinity, allow acquisition of Zn(II) at very low concentrations, when it is present as a trace element in the environment [3, 4]. The expression of the operons encoding these ABC systems is under the control of efficient Zn(II)-responsive repressors, hereafter designated as ZnRR. When Zn(II) is abundant, holo-ZnRR are active repressors avoiding unnecessary uptake. On the contrary, when Zn(II) is limiting, apo-ZnRR are inactive, allowing efficient Zn(II) uptake to maintain intra-cellular homeostasis [3, 4]. ZnRR have been identified to date in only two protein superfamilies, Ferric uptake regulator (Fur) and Multiple antibiotic resistance (MarR). Fur superfamily exclusively consists of metallo-regulators specifically involved in the control of metal homeostasis and of very few related functions [5]. The wide majority of Fur members control the homeostasis of the metallic cation they bind by repressing its uptake (Fur, Mur, Nur and Zur proteins are named according to Fe(III), Mn(II), Ni(II) or Zn(II) cations respectively), while some other ones repress the uptake of iron-containing heme, and finally PerR control oxidative stress resistance [3, 4]. In marked contrast to Fur members, MarR superfamily members regulate much more numerous and diverse physiological functions, including for example the transport of antibiotics [6, 7]. In addition, even though both Fur and MarR proteins are α-helix proteins that exist as homo-dimers, they differ by a completely different folding. In Fur proteins, the winged-helix DNA binding domain is at the N-terminus while the regulatory metal binding and dimerization regions are located at the C-terminus [8]. In marked contrast, MarR members adopt a triangular shape [9]: both the N- and C-terminal α-helices form the dimerization region, and the central globular DNA-binding domain is folded as a winged helix-turn-helix (wHTH) domain [10]. In the long-known MarR superfamily, only a few recently identified members have been shown to be metallo-regulators involved in the control of metal homeostasis, and more precisely, to be ZnRR proteins controlling Zn(II) uptake [3, 4].

ZnRR of the MarR superfamily have only been found in *Streptococcaceae*, a bacterial group including *Streptococcus* and *Lactococcus* genera, and have respectively been named AdcR [11–14] and ZitR [15, 16]. AdcR was the first MarR regulator shown to control genes encoding an ABC system for Zn(II) uptake [11, 12, 17]. In the pathogenic species *Streptococcus pneumoniae* and in the dairy species *Lactococcus lactis*, *adcR* and *zitR* regulatory genes are co-organized as operons with their *adc-zit* target genes, which encode ABC uptake systems specific for Zn(II) [11, 12, 15, 17]. In *L. lactis* subspecies *cremoris* strain MG1363, we have showed that ZitR repressor controls an emergency response to Zn(II) starvation, allowing Zn(II) uptake under extreme conditions, while impeding it in a wide concentration range, from repletion to toxicity [16]. At the molecular level, both AdcR protein of *S. pneumoniae* [14, 18] and ZitR protein of *L. lactis* subspecies *cremoris* [15, 16] have been shown to bind one or two conserved palindromic **TTAAC**YR**GTTAA** operator sites [19] in the promoter sequence of *adc*/*zit* operon and other genes. Furthermore, ZitR/AdcR proteins assemble as homo-dimers, with a stoichiometry of two cations/protomer [14, 16]. The affinity of AdcR for Zn(II) ranges from pM to nM [18]. During the course of this study, the structures of three ZnRR of the MarR superfamily have been determined. *S. pneumoniae* AdcR protein (hereafter designated as $AdcR_{Spne}$) has first been shown to be a holo-dimer with two Zn(II) ions bound per protomer [13]. *S. pyogenes* AdcR protein (hereafter designated as $AdcR_{GAS}$) has then been confirmed to be folded in a highly similar way [20]. Recently, ZitR protein of *L. lactis* subsp. *lactis* strain IL1403 (hereafter designated as $ZitR_{IL}$) has been described as a holo-dimer complexed or not to DNA [21].

This work was aimed to more deeply characterize, from a biochemical and structural point of view, ZitR protein of *L. lactis* subspecies *cremoris* strain MG1363 (hereafter designated as

$ZitR_{MG}$), which we have previously studied both *in vitro* and *in vivo* [16]. After protein production and purification in the presence of Zn(II) as previously described [16], we measured the protein stability in solution by Circular Dichroism (CD), and determined its oligomeric state by Size Exclusion Chromatography-coupled to Multi Angle Light Scattering (SEC-MALS). We also confirmed $ZitR_{MG}$ ability to bind its *zit* DNA operator site using Isothermal Titration Calorimetry (ITC). X-ray crystallography was finally used to determine the protein 3D structure. Our study allows increasing the knowledge about biophysical and structural properties of ZnRR proteins belonging to the MarR superfamily.

## Materials and methods

### ZitR purification and characterization

An untagged, recombinant (S2A, A4R, D8E) form of ZitR protein (145 amino acids, full length) from *L. lactis* subsp. *cremoris* strain MG1363 (UniProtKB/Swiss-Prot A2RNS2) was produced and purified as previously described [16]. Recombinant $ZitR_{MG}$ protein was first over-produced in *Escherichia coli* strain (BL21(DE3) (pVE8073) at 25 ˚C [16]. It was then purified in the presence of $ZnCl_2$ in two steps by anion exchange chromatography followed by heparin-affinity chromatography [16]. SDS-PAGE analysis revealed the presence of a few high molar mass contaminating *E. coli* proteins (data not shown), which could be eliminated by gel filtration chromatography in 20 mM Tris-HCl (pH 7.0), 200 mM NaCl and 100 μM $ZnSO_4$. At the end of this purification process, we observed a major dimeric form, and a minor tetrameric form (data not shown). Except for preliminary experiments (see below), only the major dimeric form has been studied and is described here. http://dx.doi.org/10.17504/protocols.io.vgye3xw.

**Matrix-Assisted Laser Desorption/Ionization—Time of flight mass spectrometry (MALDI-TOF).** For protein identification after SDS-PAGE, bands of interest were cut, submitted to trypsynolysis and analyzed using MALDI-TOF/TOF 5800 (AB Sciex) (SICaPS platform, IMAGIF). Comparison to NCBI database sequences using Mascot confirmed that the purified protein was ZitR protein from lactococcal strain MG1363 (UniProtKB/Swiss-Prot A2RNS2) (data not shown). http://dx.doi.org/10.17504/protocols.io.vgze3x6.

**Fluorescence-based Thermal Shift Assay (TSA).** Thermal stability of fully purified $ZitR_{MG}$ protein was calculated by induced thermal denaturation using a Q-PCR ABI Prism 7900HT (CTPF platform, IMAGIF). We used Sypro Orange dye, which non-specifically binds to hydrophobic surfaces and can be measured at 488 nm. Purified $ZitR_{MG}$ protein (2.5 μg) was analyzed under different conditions of buffer (Tris, phosphate, HEPES and MES), pH values (ranging from 9.2 to 4), and salt (NaCl up to 350 mM) or glycerol concentrations (up to 10%) (data not shown). http://dx.doi.org/10.17504/protocols.io.vg2e3ye.

**Size Exclusion Chromatography coupled to Multi Angle Light Scattering (SEC-MALS).** To determine the oligomeric state of $ZitR_{MG}$, 50 μl of fully purified protein at approximately 1–4 $mg.ml^{-1}$ were loaded on a KW-803 column (Shodex) equilibrated at 0.5 $ml.min^{-1}$ flow rate (Shimadzu HPLC system) and supplemented with either 1 μM $ZnSO_4$ or 1 mM EDTA (S1 Fig). Detection was performed using a MiniDAWN TREOS multi angle light scattering detector and an Optilab T-rEX differential refractometer (Wyatt Technology) (biophysics platform, LEBS/IMAGIF). Molar mass and hydrodynamic radius were calculated with the Astra 6.1.1.17 software using a differential index of refraction (dn/dc) value of 0.183 $ml.g^{-1}$. http://dx.doi.org/10.17504/protocols.io.vg3e3yn.

**Circular dichroism.** Synchrotron radiation circular dichroism (SRCD) experiments were carried out at 15 ˚C on the DISCO beamline (SOLEIL synchrotron). D-10-camphorsulfonic acid was used to calibrate the SRCD signal using the CDtool software [22]. Spectra were

obtained using calcium fluoride circular cells (Hellma) of 50 μm path length. They were loaded with $ZitR_{MG}$ protein (8 μg) in 20 mM Tris-HCl (pH 7.0), 50 mM NaCl and 100 μM $ZnSO_4$ buffer. Acquisitions at 1 nm step per second between 170 to 305 nm were recorded in triplicates. Averaged spectra were corrected with respect to the baseline by buffer subtraction and set to zero in the 300–305 nm region (S2 Fig).

Standard circular dichroism (CD) measurements were carried out at 20 ˚C on a JASCO J-810 spectropolarimeter. Temperature was controlled by a Peltier (Jasco PFD423S/L) (biophysics platform, LEBS/IMAGIF). Spectra from 185 to 260 nm were obtained using a 100 μm path length suprasil quartz cell (Hellma) containing $ZitR_{MG}$ protein (400 μg) in 20 mM Tris-HCl (pH 7.0), 50 mM NaCl and 100 μM $ZnSO_4$ buffer. All data processing was performed using CDtool software and secondary structure prediction of $ZitR_{MG}$ protein was carried out on Dichroweb server (http://dichroweb.cryst.bbk.ac.uk) using all available algorithms (CONTINLL, SELCON3, CDSSTR and K2D3) and all sets of proteins (database 1–7, SP175, SMP180) [23, 24] http://dx.doi.org/10.17504/protocols.io.vg4e3yw.

## Holo-$ZitR_{MG}$ binding to dsDNA fragments

The interaction of fully purified $ZitR_{MG}$ protein with dsDNA of different sizes (19- and 20-mers), each containing one DNA-binding domain [16, 19], was explored. Complementary oligonucleotides (from SIGMA, Eurogentec and Invitrogen) containing an imperfect **TTAAC** YR**GTTAA** palindrome overlapping either the -35 or the -10 box of the ZitR-controlled promoter region (see S1 Table for the sequences of forward oligonucleotides) were purified by SDS-PAGE or desalting. 5' overhang nucleotides (adenine in the forward oligonucleotide and thymine on the complementary one) were added to the sequence in order to make the dsDNA stickier, which might help in crystallization. Annealing of complementary forward and reverse oligonucleotides were carried out by incubation at 95 ˚C during 5 min in a 20 mM Tris-HCl (pH 8) and 150 mM NaCl buffer, followed by incubation on ice to slowly decrease the temperature.

Isothermal Titration Calorimetry (ITC) was performed on a Microcal ITC200 (GE Healthcare) (calorimetry platform, IBBMC/IMAGIF). Purified $ZitR_{MG}$ protein was dialyzed against a 20 mM Tris-HCl (pH 7.0), 150 mM NaCl and 100 μM $ZnSO_4$ buffer. Duplicate titration of approximately 20 μM $ZitR_{MG}$ protein, while stirring at 1000 rpm, was carried out by 20 injections of 2 μl of each dsDNA at 270 μM in the same buffer as the protein. The heat generated by DNA dilution was determined from the peaks measured after full saturation of the protein. Experimental data were fitted to the theoretical titration curves using the Origin software (OriginLab, Northampton, MA) according to the relationship between the heats generated by each injection. The following values were calculated: $\Delta H_{cal}$, enthalpy change in $kcal.mol^{-1}$; $K_a$, association-binding constant in $M^{-1}$; n, number of binding sites. The binding constant of each interaction is expressed as $1/K_a = K_d$ (in $mol.L^{-1}$) (S3 Fig). http://dx.doi.org/10.17504/protocols.io.vg5e3y6.

## Holo-$ZitR_{MG}$ structure determination

Holo-$ZitR_{MG}$ protein was subjected to crystallization assays using spare matrix screens in a robotic system (Nano-Robot Cartesian) (crystallography platform, LEBS/IMAGIF). In preliminary experiments, crystals were first obtained using $ZitR_{MG}$ tetrameric form by vapor diffusion in 0.2 M ammonium acetate, 0.1 M sodium citrate tribasic dihydrate (pH 5.6) and 30% polyethyleneglycol 4,000. They diffracted to a resolution of less than 6 Å. These crystals belong to $P4_1$ space group with cell parameters of $a = b = 129$ Å; $c = 88$ Å; $\alpha = \beta = \gamma = 90$˚. Crystallization conditions were then optimized using the dimeric form. X-ray data were collected at the

zinc peak absorption edge up to 3.7 Å resolution on the PROXIMA-1 beamline at SOLEIL synchrotron. After data processing by XDS [25], molecular replacement with coordinates of different MarR proteins was unsuccessful. We therefore used Zn(II) anomalous signal to solve the structure by SAD method using PHASER [26]. Eight molecules were found in the asymmetric unit, with a solvent content of 60%, and two zinc atoms were found per protomer. Phases were improved and extended by NCS averaging and solvent flattening using PARROT [27]. Refinement was done using BUSTER-TNT [28]. A low-resolution model could be built using *Bacillus subtilis* OhrR structure [29]. We could identify the extended wHTH DNA-binding domain from a poly-Ala chain, but most of the lateral chains were not visible. New data collection recorded on a Pilatus 6M detector on the same beamline went up to 2.8 Å resolution. An anisotropic correction factor was applied by STARANISO server (http://staraniso.globalphasing.org/) to sharpen the data in the weaker-diffracting direction. Structure was determined by molecular replacement using *S. pneumoniae* AdcR (3TGN) as a model [13]. The high values of average B-factors of the final structure can be explained by the crystal anisotropy. All structure figures have been created using The PyMOL Molecular Graphics System, Version 1.8 Schrödinger, LLC http://dx.doi.org/10.17504/protocols.io.vg6e3ze.

## Results and discussion

### ZitR protein of *L. lactis* subsp *cremoris* strain MG1363 is a representative member of ZnRR in the MarR superfamily

In the whole *Streptococaceae* group, ZnRR of the MarR superfamily are known to be conserved and ZitR/AdcR proteins are 48% identical (Fig 1). In the *Streptococcus* genus, AdcR proteins are slightly more conserved and display around 50% identity among species and even more within species [16]. The same holds true for lactococcal ZitR proteins, with more than 55% identity between species in the *Lactococcus* genus (e.g. more than 65% identity between *L. lactis* and *L. garvieae* proteins) and up to 89% identity between *cremoris* and *lactis* subspecies. $ZitR_{MG}$ [15, 16] appears to be a representative member of ZitR proteins among lactococcal species (Fig 1) and was chosen to be studied here. It is the fourth ZnRR of the MarR superfamily [13, 20] and the second lactococcal one [21] whose structure is determined.

### $ZitR_{MG}$ protein is a stable Zn(II)-bound dimer able to bind its DNA operator site

We produced a recombinant, untagged form of $ZitR_{MG}$ protein (145 amino acids, 16.3 kDa) in *E. coli*, purified it in the presence of Zn(II) as previously described [16], and analyzed its secondary structure. CD spectra demonstrated that purified $ZitR_{MG}$ contained a majority of helices (73.7%) and a few strands (11%). This is in agreement with $ZitR_{MG}$ protein being predicted to contain six α-helices and two antiparallel β-hairpins per protomer, as all other MarR superfamily members [7, 9]. We also determined the oligomeric state of purified $ZitR_{MG}$ by SEC-MALS. Its molar mass was found to be 32.1 ± 0.3 kDa (S1 Fig) as expected for a dimer. The protein hydrodynamic radius was found to be 2.3 ± 0.1 nm (data not shown) denoting a globular protein. EDTA, a chelator of cationic ions and in particular of Zn(II), could be added to $ZitR_{MG}$ without significantly modifying its molar mass (S1 Fig), therefore confirming that Zn (II) is not required for $ZitR_{MG}$ dimerization [16]. Overall, purified $ZitR_{MG}$ protein appeared to be both a typical MarR superfamily member, able to form stable dimers mainly folded as α-helices [6, 9], and a typical ZnRR able to bind Zn(II).

We then verified that $ZitR_{MG}$ protein was in its holo-form as expected [16]. Synchrotron Radiation CD (SRCD) spectroscopy and Fluorescence-based Thermal Shift Assay (TSA) were

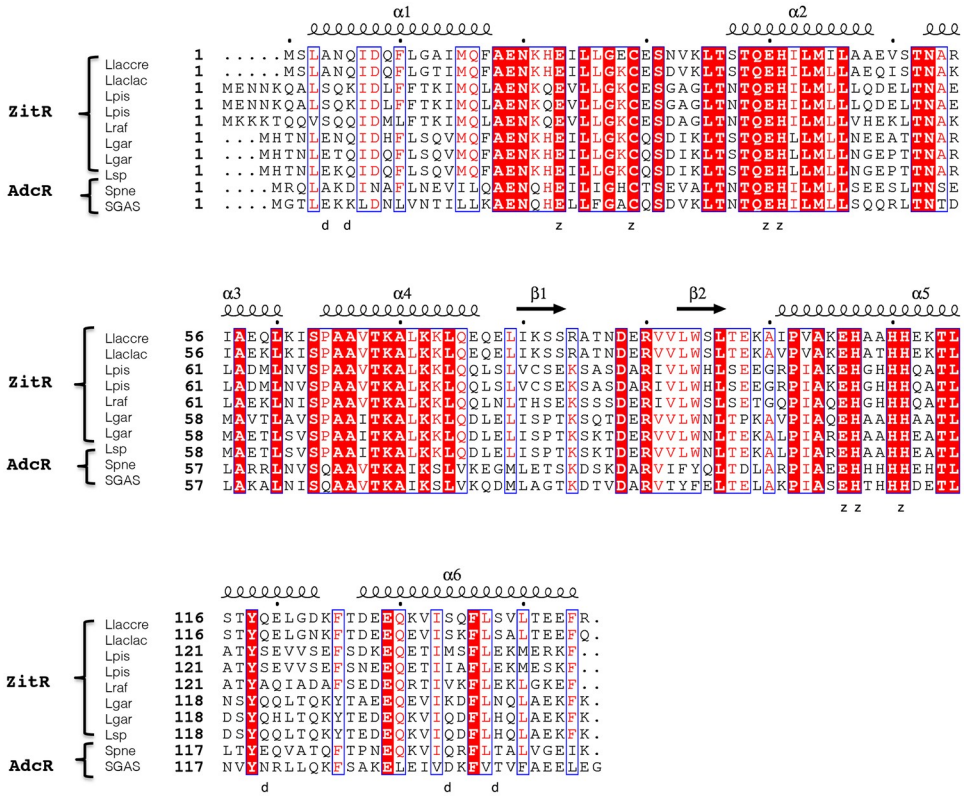


**Fig 1. Sequence conservation between ZitR/AdcR proteins.** Multi-alignment of ZitR/AdcR protein sequences was performed using Clustal Omega server (https://www.ebi.ac.uk/Tools/msa/clustalo/) and ESPript server (http://espript.ibcp.fr/ESPript/ESPript/) [30]. We noticed that several lactococcal proteins are erroneously annotated as 'AdcR' in gene/protein databases, as they share a higher homology level with ZitR proteins than to the prototypal AdcR protein from *S. pneumoniae* [13, 18, 19]. We therefore renamed them as ZitR proteins. The following sequences are shown: i) ZitR from *L. lactis* subsp. *cremoris* (Llaccre) strain MG1363 (gb |A2RNS2.1|), our lactococcal protein model [15, 16]; ii) ZitR from *L. lactis* subsp. *lactis* (Llaclac) strain IL1403 (gb |NP_268273.1|, gb |AAK06214.1|, gb |Q9CDU5|, PDB: 5YHX [21]), which is identical to ZitR proteins from *L. lactis* subsp. *lactis* strain NCDO 2118 (gb |AII13676.1|) and subsp. *lactis* bv. *diacetylactis* (gb |KZK11188.1|), not shown; iii) ZitR ('AdcR') from *L. piscium* (Lpis) strains MKFS47 (gb |CEN27435.1|) and iv) CNCM I-4031 (gb |SCA91076.1|); v) ZitR ('AdcR') from *L. raffinolactis* (Lraf) strain 4877 (gb |CCK19333.1|); vi) ZitR ('AdcR') from *L. garvieae* (Lgar) strains DCC43 (gb |EKF52529.1|) and vii) 122061 (gb |BAV02535.1|), which is identical to the protein from strain M14 (gb |CEF51164.1|), not shown; viii) ZitR ('AdcR') from *Lactococcus* sp. (Lsp) strain DD01 (gb |KXT61547.1|); ix) the prototypal AdcR protein [13, 18] from *S. pneumoniae* (Spne) strain D39 (gb |Q04I02.1|, PDB: 3TGN [13]); and finally x) AdcR protein from *S. pyogenes* strain MGAS315 (gb |AAM78676.1|), or serotype M3 (PDB: 5JLU [20]). Secondary structure elements of $ZitR_{MG}$ protein are displayed above its sequence: α-helices as medium squiggles and β-strands as arrows. $ZitR_{MG}$ residues shown here (see below) to belong to the dimerization interface or to the metal binding pocket (Fig 2) are respectively indicated by 'd' and 'z' characters below the sequences. Amino acids that appear in white characters in a red background are identical in all aligned proteins, while those in red characters and in blue frames are conserved in the majority of proteins.

https://doi.org/10.1371/journal.pone.0210123.g001

first used. Both revealed that purified $ZitR_{MG}$ protein had a high melting temperature (Tm) of around 75 ˚C, indicative of a stable protein (S2 Fig, TSA data not shown). When EDTA was added in excess to the protein, a much lower Tm of around 45 ˚C was measured by TSA (data not shown). These results confirm that purified $ZitR_{MG}$ protein is complexed to divalent (metallic) cations [16] whose binding is required for protein stability. $ZitR_{MG}$ protein has been found to be very unstable in the presence of EDTA, so that its apo-form could not be further characterized.

We also verified whether purified $ZitR_{MG}$ protein could bind DNA as expected [16]. Purified $ZitR_{MG}$ has previously been shown to be able to bind two imperfect **TTAAC**YR**GTTAA**

palindromic sequences (with the two 5 bp-inverted repeats in bold) that are present in *zit* promoter (P*zit*) and overlap its -35 and -10 boxes [16]. Two double-stranded (ds) small DNA fragments, each containing one palindromic sequence, were designed to perform binding assays using purified $ZitR_{MG}$ (S1 Table). ITC experiments confirmed, as expected, that $ZitR_{MG}$ protein was able to bind its two palindromic sequences (S3 Fig) [16]. They also revealed positive enthalpy changes (ΔH), indicating that $ZitR_{MG}$ interaction with dsDNA fragments is an endothermic and entropically driven process that implies a hydrophobic component in the binding.

## Crystal structure of holo-$ZitR_{MG}$ protein

The structure of $ZitR_{MG}$ holo-form was first determined at low resolution by single anomalous wavelength dispersion (SAD) and then, after crystal improvement by molecular replacement, at 2.8 Å resolution. The asymmetric unit (ASU) contained 8 $ZitR_{MG}$ molecules, and 16 Zn(II) atoms. $ZitR_{MG}$ molecules formed four dimers (AB, CD, EF and GH), all binding four Zn(II) atoms in total (two per protomer). Crystallographic data and refinement statistics are summarized in Table 1. Three of the dimers were almost identical, with all 2290 atoms root-mean-square-deviation (RMSD) values ranging from 0.34 Å (AB/CD) to 0.50 Å (AB/GH). Dimer EF was less defined (with high all 2290 atoms RMSD values, at least 1.37 Å (AB/EF) and up to 1.44 Å (EF/GH)). AB dimer was chosen as a $ZitR_{MG}$ dimer prototype and is described in the following. In AB, both protomers have almost the same conformation and superimpose to each other with all 1144 atoms-RMSD of 0.34 Å. Each protomer is arranged from the N- to the C-terminus as follows: α1 (residues 3–17), α2 (residues 37–48), α3 (residues 53–60), α4 (residues 64–77), β1 (residues 80–83), β2 (residues 93–96), α5 (residues 100–124) and α6 (residues 127–144) (Fig 1), in good agreement with our above-mentioned CD results, and as expected for a typical MarR superfamily member [7, 9].

$ZitR_{MG}$ protein is folded as a triangular-shaped homo-dimer with a two-fold pseudo-symmetric axis (Fig 2A), a typical topology for a MarR superfamily member [7, 10]. It best matches $ZitR_{IL}$ holo-dimer, but it also well aligns to the DNA-bound form of $ZitR_{IL}$ [21], the holo-form of streptococcal AdcR proteins [13, 20], and finally non-ZnRR members of the MarR superfamily (Table 2) (S4A and S4B Fig). Each monomer of $ZitR_{MG}$ protein contains three well-defined regions (in grey in Fig 2A): a dimerization interface, a wHTH DNA-binding domain and a metal-binding pocket, which are described in the following sections.

**Protomers interact via hydrogen bonds in the dimerization interface.** The dimerization interface involves the N- and C-terminus of $ZitR_{MG}$ protein, as in $ZitR_{IL}$ [21] and AdcR proteins [13, 20]. In $ZitR_{MG}$ dimerization interface, the N-terminal α1 helix (protomer A), which is stacking between α5'-α6' helices, interacts with α1', its counterpart in protomer B, and the same holds true for the C-terminal α6 and α6' helices (Figs 1 and 2A). These interactions are mainly through four hydrogen bonds (Fig 2B). Three of them, involving the following atom pairs: Nε2-Gln6 (α1) and main chain O-Ser134', Nε2-Gln6 and Oγ-Ser138' (α6'), and finally Oε1-Gln6 (α1) and Oγ-Ser134' (α6'), are conserved in $ZitR_{IL}$ protein, while the fourth, NH1-Arg4 (α1) and Oε1-Gln119' (α5'), is specific to the recombinant $ZitR_{MG}$ protein (see Materials and methods section). AdcR proteins display three completely different hydrogen bonds. They involve: i) NZ-Lys7 (α1) and Oδ1-Asp135' (α6'), Oε1-Glu20 (loop α1-α2) and N-Asn38' (α2), and finally Oε2-Glu20 (loop α1-α2) and Oγ1-Thr39' (α2), in the case of $AdcR_{GAS}$ [20]; and ii) N-Arg2 (α1) and Oε1-Glu120' (α5'), Nε-Arg2 (α1) and Oε1-Gln131' (α6'), and finally Oε2-Asp7 (α1) and Nε2-Gln135 (α6'), in the case of $AdcR_{Spne}$ [13]. In $ZitR_{MG}$ dimer, the hydrogen bonds in the dimerization interface are probably involved in

**Table 1. Crystallographic data and statistics.**

| | |
|---|---|
| ***Data Collection*** | |
| Space group | P 41 |
| *a*, *b*, *c* (Å) | 128.52, 128.52, 88.14 |
| α,β,γ (˚) | 90, 90, 90 |
| Wavelength (Å) | 1.28189 |
| Resolution (Å) | 48.15–2.8 (2.975–2.872)[h] |
| No. of observed reflections | 43447 (1029)[h] |
| No. of unique reflections | 21630 (515)[h] |
| Multiplicity | 2.0 (2.0)[h] |
| $R_{merge}$ (%)[a] | 6.722 (51.34)[h] |
| $R_{meas}$ (%)[b] | 9.506 |
| Completeness (%) | 65.60 (13.34)[h] |
| I/σ[c] | 16.62 (1.62)[h] |
| $CC_{1/2}$[d] | 0.994 (0.392)[h] |
| CC*[e] | 0.998 (0.751)[h] |
| ***Refinement*** | |
| $R_{work}$ (%)[f] | 23.65 |
| $R_{free}$ (%)[g] | 25.14 |
| Number of non-hydrogen atoms | 9168 |
| in macromolecules | 9152 |
| in ligands | 16 |
| Protein residues | 1152 |
| RMS bond deviation (Å) | 0.012 |
| RMS angle deviation (˚) | 1.57 |
| Ramachandran favored (%) | 97.98 |
| Ramachandran allowed (%) | 2.02 |
| Ramachandran outliers (%) | 0 |
| Clashcore | 3.08 |
| Average B-factor | 162.20 |
| in macromolecules | 162.20 |
| in ligands | 160.60 |

[a]Rmerge = $\Sigma_{hkl}\Sigma_j|I_{hkl,j}-<I_{hkl}>|\Sigma_{hkl}\Sigma_i I_{hkl,j}$

[b]Rmeas = $\Sigma_{hkl}\sqrt{n/n-1}\ \Sigma^{v}_{j=1}|I_{hkl}-<I_{hkl}>|\Sigma_{hkl}\Sigma_i|I_{hkl,j}$

[c]I/ σ = signal-to-noise ratio

[d]$CC_{1/2}$ = Pearson correlation coefficient

[e]$CC^* = \sqrt{2CC_{1/2}/1+CC_{1/2}}$

[f]Rwork = $\Sigma_{hkl}||Fobs(hkl)|-k|Fcalc(hkl)||/\ \Sigma_{hkl}|Fobs(hkl)$

[g]Rfree = $\Sigma_{hklCT}||Fobs(hkl)|-k|Fcalc(hkl)||\ \Sigma_{hklCT}|Fobs(hkl)$

[h]Values in parenthesis correspond to the last resolution shell

https://doi.org/10.1371/journal.pone.0210123.t001

protein stability, as it is the case in the other ZitR/AdcR proteins of determined structure [13, 20, 21].

In the overall $ZitR_{MG}$ structure, the dimerization interface and the DNA-binding domain are connected *via* the α2 and α5 helices (Fig 2A), as it is also the case in other MarR superfamily members [10].

**The DNA-binding domain is structurally conserved between $ZitR_{MG}$ and other MarR superfamily members.** In $ZitR_{MG}$ like in *E. coli* MarR [10], streptococcal AdcR proteins [13,

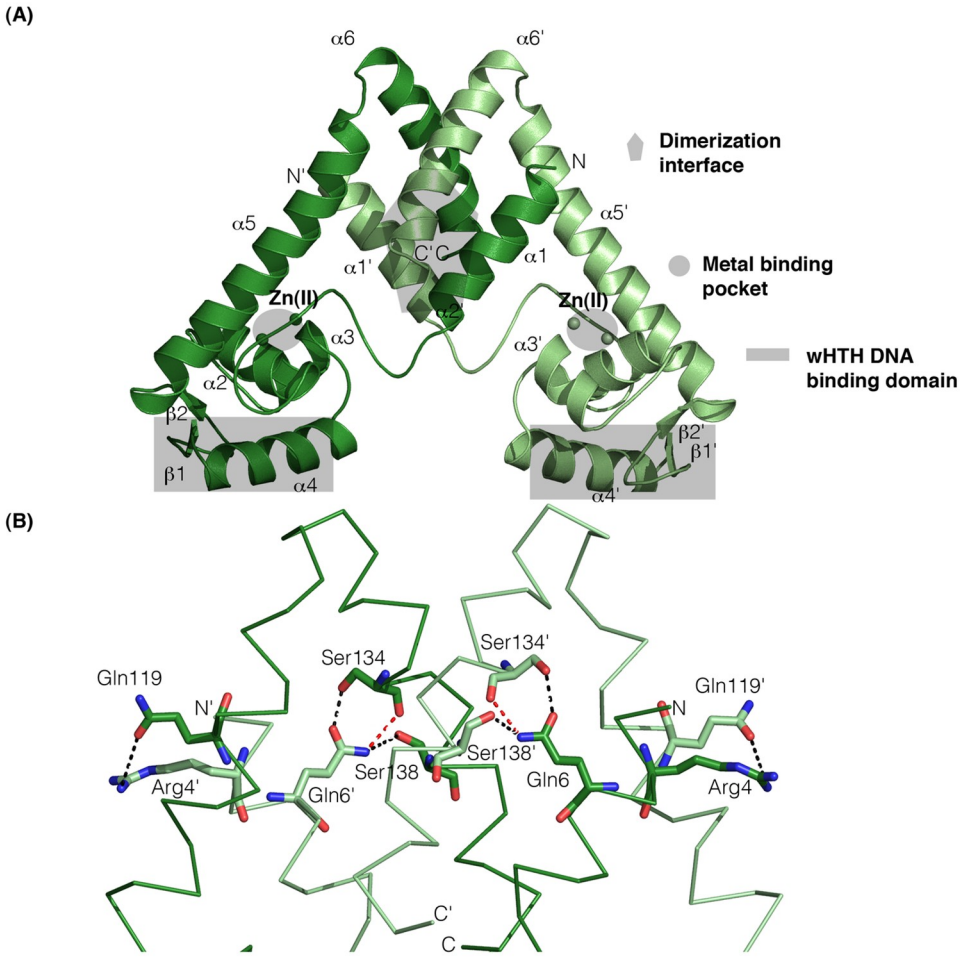


**Fig 2. Structure of holo-ZitR$_{MG}$ dimer.** (A) Overall structure. Protomers A and B of ZitR$_{MG}$ dimer, represented in ribbon, are colored in dark and light green respectively, and their N- and C-terminus are indicated. Zn(II) atoms are shown as small green spheres. Helices and strands are labelled. The dimerization interface, each wHTH DNA-binding domain and each metal-binding pocket are indicated by different forms colored in grey, respectively a polygon, a rectangle and a circle. (B) Close view of dimer interface. Protomers A and B of ZitR$_{MG}$ dimer are shown as in Fig 2A. Residues involved in dimerization are labelled and represented in ball-and-sticks, with N atoms colored in blue and O atoms in red. Hydrogen bonds are shown as dashed lines, either in black in most cases or in red when they involve main chain atoms.

https://doi.org/10.1371/journal.pone.0210123.g002

20] and ZitR$_{IL}$ [21], the DNA-binding domain is folded as a wHTH domain made of a helix region (formed by α2, α3 and α4 helices) and a β strand region (β1 and β2 strands) (Fig 2A and S4A and S4B Fig). In all proteins of the MarR superfamily, these two regions are respectively involved in the binding of the DNA major and minor grooves [9]. The α4 helix and the β1 strand form an angle of approximately 30 ˚ in each ZitR$_{MG}$ protomer, as it is the case in the other ZitR/AdcR proteins [13, 20, 21]. This conformation is widely conserved in MarR superfamily and probably allows DNA accommodation and binding [9].

In order to get insights about DNA-binding ability of ZitR$_{MG}$, we compared its 3D fold to that of the three MarR members whose structure had been determined in both DNA-bound or DNA-free conformations at that time (and later also to that of ZitR$_{IL}$ [21]): *Yersinia pseudotuberculosis* RovA [31], *Salmonella enterica* SlyA [32], and *B. subtilis* OhrR [29] (Table 2). It is worth noting that in these three proteins, DNA-binding activity is not induced by the binding of a ligand, in contrast to the situation in the best known superfamily member, *E. coli* MarR [9,

**Table 2. Structure comparison between $ZitR_{MG}$ protein and other MarR superfamily members.**

| Protein or Protein/ DNA complex (PDB) | Species | Protein Identity to $ZitR_{MG}$ (%) | r.m.s.d over all atoms protomer | r.m.s.d over all atoms dimer | Reference |
|---|---|---|---|---|---|
| $ZitR_{MG}$ (this study, 6FI9) | *L. lactis* subsp. *cremoris* (strain MG1363) | 100 | 0.34 | ***Not Applicable*** | This study |
| $ZitR_{IL}$ (5YHX) | *L. lactis* subsp. *lactis* (strain IL1403) | 89 | 1.76 | **1.18**[a] | [21] |
| $ZitR_{IL}$/16-mer DNA (5YI2) | | | 2.41 | **2.30**[a] | |
| $AdcR_{Spne}$ (3TGN) | *S. pneumoniae* | 47 | **1.65**[a] | 2.76 | [13] |
| $AdcR_{GAS}$ (5JLS) | *S. pyogenes* | 44 | **3.35**[a] | 6.01 | [20] |
| $AdcR_{GAS}$ (C-terminally His tagged, 5JLU) | | | **4.07**[a] | 6.42 | |
| OhrR/29-mer DNA (1Z9C) | *B. subtilis* | 23 | **5.87**[a] | 6.51[b] | [29] |
| OhrR (1Z91) | | | **17.03**[a] | 17.16 | |
| RovA /21-mer DNA (4AIJ) | *Y. pseudotuberculosis* | 24 | **4.83**[a] | 6.09 | [31] |
| RovA (4AIH) | | | **5.28**[a] | 7.19[b] | |
| SlyA/23-mer DNA (3Q5F) | *S. enterica* | 22 | **4.91**[a] | 6.06 | [32] |
| SlyA (3QPT) | | | **5.37**[a] | 8.17 | |

[a]For each comparison the best RMSD value is in bold.

[b]When several dimers are present in the asymmetric unit of a protein crystal (ohrA-bound OhrR (1Z9C) and DNA-free RovA (4AIH)) only the AB dimer is considered in this Table.

https://doi.org/10.1371/journal.pone.0210123.t002

10]. Indeed, RovA and OhrR, which do not bind any ligand, acquire their DNA-binding activity upon a conformational change induced by a temperature [31] or oxygen shift respectively [29, 33], while in SlyA, the salicylate ligand and DNA compete for the same binding site [32]. Interestingly, $ZitR_{MG}$ is shown here to better align to the DNA-bound form of any MarR protein than to its DNA-free counterpart (Table 2), suggesting that holo-$ZitR_{MG}$ dimer could be folded in a DNA-binding prone conformation. Consistently, we previously showed by EMSA [16] that Zn(II) binding is required for the DNA-binding activity of purified $ZitR_{MG}$ dimer, as also shown for AdcR proteins [14, 34]. In addition, in $ZitR_{IL}$ protein, both DNA-bound and DNA-free holo-forms share a highly similar structure that is different from that of the apo-form [21], showing that only the holo-form is in a DNA-binding prone conformation. Finally, in ZnRR proteins of the MarR superfamily, activity is acquired upon the binding of the ligand, as it is the case for a distantly related, non ZnRR superfamily member, *E. coli* MarR. In this protein, ligand binding changes the orientation of the two DNA recognition regions and their distance in the wHTH domain [9].

In $ZitR_{MG}$ wHTH domain, we noticed that $Arg90_{ZitR}$, a highly exposed residue, protrudes at the protein surface (Fig 3, S5A and S5B Fig), suggesting that it could interact with DNA. Noteworthy, $Arg90_{ZitR}$ is widely conserved in all members of the MarR superfamily, including OhrR [29], RovA [31], SlyA [32], AdcR [13, 20] and $ZitR_{IL}$ [21] (Fig 1 and S6 Fig), and this conserved Arg residue has been shown, in two superfamily members, MarR and MexR proteins, to be required for full DNA-binding activity *in vitro* [10, 35]. Furthermore, in the DNA-bound form of RovA [31], SlyA [32] and OhrR [29], this conserved Arg has been found to contact the DNA minor groove. This contact can neither be observed in DNA-bound $ZitR_{IL}$, as DNA is too short, nor can it be excluded [21]. In OhrR [29], $Asp92_{OhrR}$, which is also widely conserved in the whole MarR superfamily, notably in RovA [31], SlyA [32] and ZitR/AdcR proteins [13, 20, 21], has been shown to strengthen the interaction between $Arg94_{OhrR}$ and DNA. In $ZitR_{MG}$, the conserved Arg residue ($Arg90_{ZitR}$) could therefore be located in the

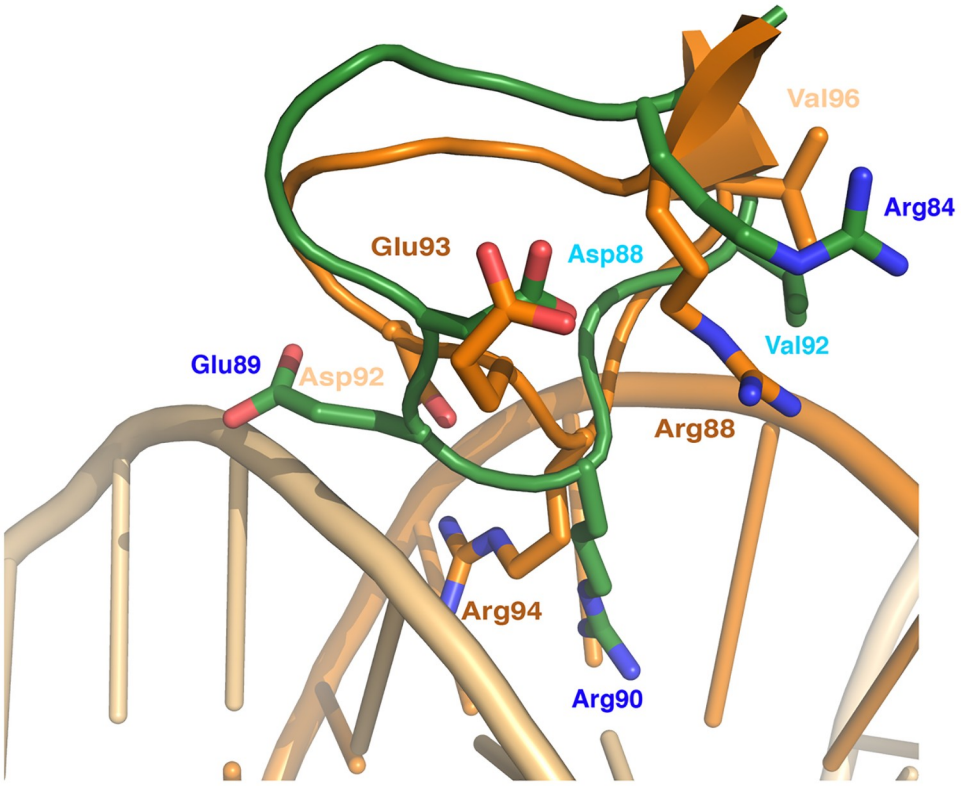


**Fig 3. The wHTH DNA-binding domain of $ZitR_{MG}$.** The structure of holo-$ZitR_{MG}$ protein (this study, 6FI9, protomer A is shown as a green ribbon) and that of OhrR-*ohrA* complex (1Z9C, OhrR protomer A is shown as an orange ribbon and *ohrA* DNA colored in light-orange) have been superimposed, and a zoom on the Arg94 of OhrR wHTH DNA-binding domain is shown. Residues aligned between $ZitR_{MG}$ and OhrR are represented as ball-and-sticks with N colored in blue and O in red. Fully and moderately accessible residues are labelled in dark and light color respectively.

https://doi.org/10.1371/journal.pone.0210123.g003

DNA minor groove with the help of the conserved Asp residue ($Asp88_{ZitR}$). Besides, in OhrR, these two residues form a small cluster with three very close residues also contacting the DNA minor groove, $Arg88_{OhrR}$, $Glu93_{OhrR}$ and $Val96_{OhrR}$ [29]. Interestingly enough, these three residues are specifically conserved in the sequences of $ZitR_{MG}$ and $ZitR_{IL}$ proteins (as $Arg84_{ZitR}$, $Glu89_{ZitR}$ and $Val92_{ZitR}$ in $ZitR_{MG}$), but not in that of other ZitR/AdcR proteins (Fig 1) or other MarR members (S6 Fig). In structure superimposition, they align between $ZitR_{MG}$ and either OhrR (Fig 3) or $ZitR_{IL}$ (S5 Fig), suggesting that the whole cluster around the Arg residue in the two crystallized ZitR proteins could define a wHTH region interacting with DNA minor groove. Finally, another $ZitR_{MG}$ residue, $Thr36_{ZitR}$ (loop α1-α2), both highly exposed at the protein surface and conserved in MarR superfamily members (S6 Fig), could also contact DNA by alignment to the conserved and DNA-contacting Thr residue in OhrR [29], RovA [31] and SlyA [32]. This Thr residue has indeed recently been confirmed to contact DNA in $ZitR_{IL}$ [21].

Few residues are involved in DNA major groove contacts in MarR proteins, and they are generally not conserved. A Thr residue conserved between $ZitR_{MG}$ and OhrR sequences (S6 Fig) and structures (data not shown), $Thr68_{ZitR}$, could be involved in such a contact. Indeed, in OhrR, its counterpart, $Thr72_{OhrR}$ (α4), is known to interact with the DNA phosphate backbone of the major groove, *via* a main chain hydrogen interaction [29]. This Thr residue, which is also widely conserved among ZitR/AdcR sequences (Fig 1), has recently been confirmed to

contact DNA major groove in the DNA-bound $ZitR_{IL}$ [21], highly suggesting that it could have the same role in $ZitR_{MG}$. In conclusion, structure superimposition to the available DNA-bound MarR proteins allowed us predicting $ZitR_{MG}$ residues putatively involved in DNA binding, even though further experiments will be required to demonstrate their role.

The DNA-binding domain of $ZitR_{MG}$ is connected to the Zn(II)-binding pocket by a hydrogen-bonding network, between α2 and α4 helices (Fig 2A), as is also the case in other MarR proteins [10].

**The Zn(II)-binding pocket show subtle differences between ZitR and AdcR.** The Zn(II)-binding pocket is made up by α2 and α5 helices, together with the extended α1-α2 loop of each protomer (Fig 1). Most residues involved in Zn(II) binding (see below) were buried or moderately exposed (S6 Fig), in marked contrast to residues proposed by structure alignment to be involved in DNA binding (see above). The two metal binding sites of $ZitR_{MG}$ protein, like those of $ZitR_{IL}$ [21] and $AdcR_{Spne}$ [13], are located at opposite sides of the dimer and two Zn(II) ions are bound per protomer (Fig 2A, S4A and S4B Fig). At a first glance, the Zn(II)-binding sites of $ZitR_{MG}$, $ZitR_{IL}$ and $AdcR_{Spne}$ proteins are highly similar, even though the internuclear Zn(II)-Zn(II) distance is shorter in $ZitR_{MG}$ (7.3 Å -7.6 Å for protomers A and B; Fig 4A) than in $ZitR_{IL}$ or $AdcR_{Spne}$ (7.9 Å—8.1 Å for protomers A and B in both proteins; S7A and S7D Fig; only one Zn(II) ion per protomer could be determined in $AdcR_{GAS}$ structure [20]). Zn(II)-coordinating residues are conserved and organized as globally similar binding sites between the two proteins (see below).

The Zn(II)-binding site 1 of $ZitR_{MG}$ is composed of four residues conserved in ZitR/AdcR proteins (Fig 1). $Glu23_{ZitR}$, $His41_{ZitR}$ and $His111_{ZitR}$ are moderately exposed, while $His107_{ZitR}$ is buried (S6 Fig). Zn(II) is clearly coordinated by $O\varepsilon1\text{-}Glu23_{ZitR}$, $N\delta1\text{-}His41_{ZitR}$, $N\varepsilon2\text{-}His107_{ZitR}$ and $N\varepsilon2\text{-}His111_{ZitR}$, although a supplementary coordination involving a second atom of the first ligand ($O\varepsilon2$) has also been proposed in $AdcR_{Spne}$ (see below) (Fig 4B; Table 3A). Our data are in good agreement with what has been observed for $AdcR_{Spne}$ [13] and $ZitR_{IL}$ [21], while in $AdcR_{GAS}$ [20], only the last three ligands have been determined together with three water molecules (Table 3). In $AdcR_{Spne}$, Zn(II) has been described as tetrahedrally coordinated by $O\varepsilon1\text{-}Glu24_{AdcR}$, $N\delta1\text{-}His42_{AdcR}$, $N\varepsilon2\text{-}His108_{AdcR}$ and $N\varepsilon2\text{-}$

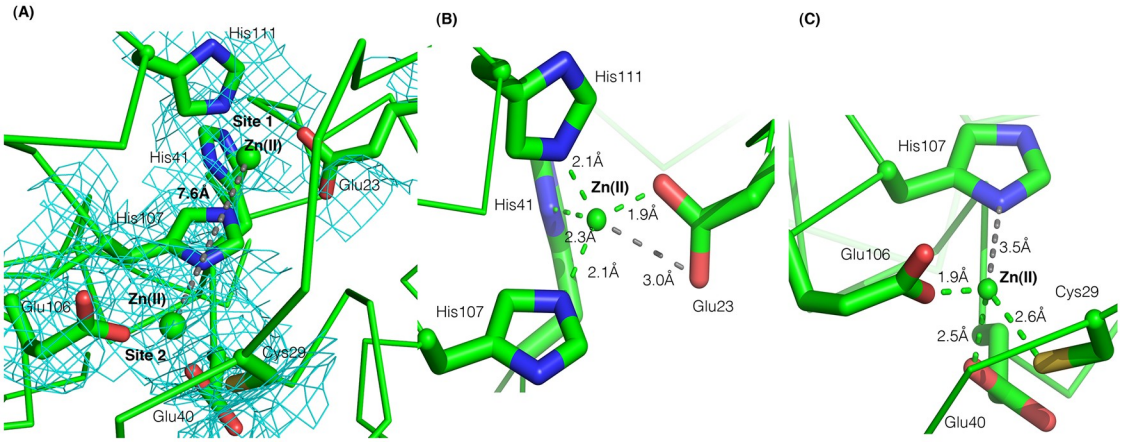


**Fig 4. The Zn(II) metal binding pocket of holo-$ZitR_{MG}$ dimer.** Only the protomer A is shown in green. Zn(II) atoms are represented as small green spheres and their ligands as ball-and-sticks, with their N, O and S atoms respectively colored in blue, red and yellow. (A) Electron density map of the whole Zn(II) binding pocket. 2Fo-Fc contoured at 1.0σ is displayed as a cyan mesh. Internuclear Zn(II)-Zn(II) distance is indicated close to a grey dashed line between Zn(II) atoms. (B) Zn(II) binding site 1 and (C) Zn(II) binding site 2. Coordination bonds are represented as green dashed lines. A grey dashed line is shown between a residue atom and a Zn(II) atom when their distance is $\geq$ 3 Å.

https://doi.org/10.1371/journal.pone.0210123.g004

**Table 3. Comparison of Zn(II) coordination in ZnRR proteins.**

| A<br>Zn(II)-binding site 1 | | | | | | | |
|---|---|---|---|---|---|---|---|
| **$ZitR_{MG}$** | **Å** | **$ZitR_{IL}$** | **Å** | **$AdcR_{Spne}$** | **Å** | **$AdcR_{GAS}$** | **Å** |
| **Oε1-Glu23** | **1.9** | **Oε1-Glu24** | **2.3** | **Oε1-Glu24** | **2.0** | Oε1-Glu24 not determined | ***Not Applicable*** |
| Oε2-Glu23 | 3.0 | Oε2-Glu24 | 2.9 | Oε2-Glu24[a] | 2.8 | Oε2-Glu24<br>not determined | ***Not Applicable*** |
| **Nδ1-His41** | **2.3** | **Nδ1-His42** | **2.0** | **Nδ1-His42** | **2.0** | *Nδ1-His42* | *4.1*[b] |
| *Nε2-His41*[c] | *4.3*[b] | *Nε2-His42*[c] | *4.1*[b] | *Nε2-His42* | *4.1*[b] | **Nε2-His42**[c] | **2.4** |
| **Nε2-His107** | **2.1** | **Nε2-His108** | **2.0** | **Nε2-His108** | **2.1** | **Nε2-His108** | **2.3** |
| **Nε2-His111** | **2.1** | **Nε1-His112** | **2.1** | **Nε1-His112** | **2.0** | **Nε1-His112** | **2.3** |
| | | | | | | 3 $H_2O$ | **2.0, 2.2, 2.2** |
| **B**<br>Zn(II)-binding site 2 | | | | | | | |
| **$ZitR_{MG}$** | **Å** | **$ZitR_{IL}$** | **Å** | **$AdcR_{Spne}$** | **Å** | **$AdcR_{GAS}$** | **Å** |
| **S-Cys29** | **2.6** | **S-Cys30** | **2.5** | **S-Cys30** | **2.3** | S-Cys30 | ***Not Applicable***<br>***No Zn(II)*** |
| **Oε1-Glu40** | **2.5** | **Oε1-Glu41** | **2.2** | **Oε1-Glu41** | **2.0** | Oε1-Glu41 | ***Not Applicable***<br>***No Zn(II)*** |
| **Oε1-Glu106** | **1.9** | **Oε1-Glu107** | **2.0** | **Oε1-Glu107** | **2.0** | Oε1-Glu107 | ***Not Applicable***<br>***No Zn(II)*** |
| | | $H_2O$ | 1.8 | $H_2O$ | 2.1 | | |

The distance between a zinc atom and each of its ligands is indicated for each site (site 1 in A and site 2 in B) of the following ZnRR proteins of the MarR superfamily: $ZitR_{MG}$ (this study, 6FI9), $ZitR_{IL}$ (5YHX), $AdcR_{Spne}$ (3TGN) and $AdcR_{GAS}$ (5JLS).

[a]Oε2-Glu24 has been proposed in $AdcR_{Spne}$ to be a putative fifth ligand for Zn(II) in the binding site 1 [13] according to X-ray absorption spectroscopy data [18].

[b]Ligands whose distance to Zn(II) atom is > 3 Å are indicated in italic.

[c]Nε2-His42 is the Zn(II) ligand in $ZitR_{IL}$ site 1 only when site 2 is not occupied, and switches to Nδ1-His42 upon binding of a second Zn(II) to site 2 [21]. Nε2-His42 in $AdcR_{GAS}$ [20] is closer to Zn(II) bound in site 1 than Nδ1-His42.

https://doi.org/10.1371/journal.pone.0210123.t003

$His112_{AdcR}$ (S7B and S7E Fig; Table 3A) [13]. However, as previous X-ray absorption spectroscopy data had indicated that Zn(II) could be penta-coordinated in binding site 1 of $AdcR_{Spne}$ [18], careful examination of 3D structure data revealed Oε2-$Glu24_{AdcR}$ as a possible supplementary ligand. Indeed, $Glu24_{AdcR}$ was proposed to be able, by a relatively small movement of its side chain, to achieve a bi-dentate coordination of Zn(II) *via* both Oε1 and Oε2, thus finally leading to Zn(II) penta-coordination [13]. Interestingly, the internuclear distances between the Zn(II) atom and each of its coordination residues are highly conserved among $ZitR_{MG}$, $ZitR_{IL}$ and $AdcR_{Spne}$ proteins (Table 3A). Zn(II)-binding site 1 is therefore highly conserved between ZitR/AdcR proteins and contains at least four ligands (Oε1-Glu23, Nδ1-His41, Nε2-His107 and Nε2-His111 in $ZitR_{MG}$), and possibly also a fifth one (Oε2-Glu23 in $ZitR_{MG}$; Fig 4B, S7B and S7E Fig; Table 3A). Zn(II)-binding site 1 therefore displays the same geometry in all ZitR/AdcR proteins, even though its nature cannot yet be defined without ambiguity. Depending on whether Zn(II) is tetra- or penta-coordinated, Zn(II)-binding site 1 could respectively display a trigonal bipyramidal or a distorted tetrahedral geometry, as previously discussed in the case of $AdcR_{Spne}$ [13]. Finally, our and previous structural data on $ZitR_{MG}$ (this study), $ZitR_{IL}$ [21] and $AdcR_{Spne}$ [13, 18] are highly consistent.

Overall, the Zn(II) binding site 2 is also well conserved among ZitR/AdcR proteins. The three Zn(II) ligands in $ZitR_{MG}$ site 2: SH-$Cys29_{ZitR}$, Oε1-$Glu40_{ZitR}$ (a buried residue, S6 Fig), and Oε1-$Glu106_{ZitR}$ (Figs 1 and 4C; Table 3B), are the same as in $ZitR_{IL}$ and $AdcR_{Spne}$ (S7C and S7F Fig; Table 3B). The unique Cys residue of ZitR/AdcR proteins (SH-Cys29 in $ZitR_{MG}$)

is therefore confirmed to be a Zn(II) ligand in $ZitR_{MG}$ (this study) like in $ZitR_{IL}$ [13, 21], and $AdcR_{Spne}$ [13], in contrast to initial findings for the latter protein [18]. Yet, a water molecule, which is used as a fourth Zn(II) ligand in $AdcR_{Spne}$ [13] and $ZitR_{IL}$ [21], has not been observed here in $ZitR_{MG}$. It cannot be excluded (Table 3B) that such a water molecule could be part of Zn(II)-binding site 2 in $ZitR_{MG}$ under other conditions. Alternatively, as the distance between the Zn(II) atom of site 2 and one His residue of site 1 is slightly smaller in $ZitR_{MG}$ (3.5 Å for Zn(II)- $His107_{ZitR}$) (this study) than in $ZitR_{IL}$ (4.0 Å for Zn(II)-$His108_{ZitR}$) [21] or $AdcR_{Spne}$ (4.1 Å for Zn(II)-$His108_{AdcR}$) [13]) (Table 3B), the whole Zn(II)-binding pocket could display subtle folding differences among ZitR/AdcR proteins.

The mechanism of Zn(II)-binding and its effect on DNA-binding have recently been clarified in $ZitR_{IL}$. In this protein, the binding of a second Zn(II) atom at site 2 involved a switch in Zn(II) coordination at the high affinity site 1, between the two nitrogen atoms of His42, leading to the reorganization of the wHTH domain into an optimal DNA-binding conformation [21]. The binding cooperativity between the two Zn(II) binding sites enables $ZitR_{IL}$ to adapt to a broad range of zinc fluctuation that results in a fine-tuned control of transcriptional regulation. In other MarR proteins, like $AdcR_{Spne}$, the two Zn(II) sites have also been found to display different affinities, and the high and low affinity sites were respectively proposed to be a regulatory site and a site of unknown function [13, 18]. In $ZitR_{MG}$ (this study), Zn(II) binding site 2 could serve to modulate DNA-binding activity, as proposed for $AdcR_{Spne}$ [13]. Alternatively, as our previous *in vivo* data indicate that $ZitR_{MG}$ functions as a repressor in a wide concentration range, from repletion to toxicity [16], Zn(II) binding at site 2 could allow modulating gene expression in response to high to toxic Zn(II) concentrations, in $ZitR_{MG}$ like in $ZitR_{IL}$ [21]. Further studies would be needed to definitely establish the function of Zn(II) binding in $ZitR_{MG}$ protein.

Intriguingly, similar properties have also been described for Zur metallo-regulators belonging to the Fur superfamily and used by most bacterial species. In *Streptomyces coelicolor* Zur protein, there are two regulatory sites (M and D) that regulate DNA-binding in different ways, by an on-off switch and a fine-tuner respectively [36]. In *B. subtilis* Zur protein, there is a sequential negative binding cooperativity between the regulatory Zn(II) binding sites, possibly allowing this protein to sense a broader range of intracellular Zn(II) concentrations [37]. Understanding why gene regulation by Zn(II) is performed by ZitR/AdcR proteins in the *Streptococaceae* group and Zur proteins in almost all other bacterial species will deserve further investigations.

## Conclusions

In this study, we have characterized $ZitR_{MG}$, a metallo-regulator of the MarR superfamily. In solution, $ZitR_{MG}$ has been shown to be a stable dimer able to bind, as expected [16], both Zn (II) and double-stranded DNA fragments bearing the palindromic **TTAAC**YR**GTTAA** recognition sequence [16, 19]. We have determined the structure of holo-$ZitR_{MG}$ by X-ray crystallography. $ZitR_{MG}$ is the fourth ZnRR in MarR superfamily whose structure has been determined. The overall 3D fold of $ZitR_{MG}$ best matches that of $ZitR_{IL}$ [21], is highly similar to that of $AdcR_{Spne}$ [13] and, to a lesser extent, to that of $AdcR_{GAS}$ [20], and is related to that of other MarR members.

Interestingly, when holo-$ZitR_{MG}$ and a few Zn(II)-independent regulators of the MarR superfamily have been compared, the former has been found to be closer to DNA-bound state of the MarR members than to its DNA-free state. This suggests that Zn(II) binding could drive modifications of the quaternary structure to efficiently accommodate DNA in $ZitR_{MG}$, as previously shown in *E.coli* MarR proteins [9] and recently in $ZitR_{IL}$ [21].

## Supporting information

**S1 Table. $ZitR_{MG}$ DNA-binding as revealed by ITC experiments.**
(PDF)

**S1 Fig. Purified $ZitR_{MG}$ is a dimer.** SECMALS analysis of untreated (in black) and EDTA-treated $ZitR_{MG}$ protein (in red) using a KW-803 column. Elution profiles are represented as a function of the molar mass. The molar mass and the hydrodynamic radius of EDTA-treated $ZitR_{MG}$ have been calculated from light scattering and refractometry data and found to be 32.1 ± 0.3 kDa and 2.3 ± 0.1 nm, respectively.
(TIF)

**S2 Fig. Purified $ZitR_{MG}$ is a stable protein.** $ZitR_{MG}$ has been characterized by circular dichroism (CD): Ellipticity (θ) in millidegrees (mdeg) is shown as a function of the wavelength (from 190 to 270 nm). CD temperature scans by steps of 10 ˚C, from 20 ˚C to 80 ˚C are shown (the color of the scan is different as a function of the temperature, and the correspondence is shown on the right). In the insert, ellipticity (θ) in millidegrees (mdeg) is shown as a function of temperature at either 208 nm (full square) or 222 nm (empty square). The inflexion point of both curves is the $ZitR_{MG}$ melting temperature (Tm), and it is of around 75 ˚C.
(TIF)

**S3 Fig. Purified $ZitR_{MG}$ is able to bind palindromic double-stranded DNA fragments.** ITC measurements of $ZitR_{MG}$ interaction with two different palindromic dsDNA fragments. (A) Palindrome 1 overlapping the -35 box of *Pzit* promotor and (B) Palindrome 2 overlapping the -10 box of *Pzit* promotor (see S1 Table for the sequences of forward oligonucleotides). The top panels show the raw data, the heat (microcalories.second$^{-1}$) generated by each injection of DNA during titration experiments as a function of time (minutes). The bottom panels show the binding isotherms created by plotting the heat as a function of protein concentration and the fitting to theoretical curves. A representative experiment is shown in each case. These figures have been created with Origin (OriginLab, Northampton, MA).
(TIF)

**S4 Fig. Structure conservation between ZnRR holo-dimers in the MarR superfamily.** The structure of $ZitR_{MG}$ holo-dimer (this study, 6FI9, in green) and that of either (A) $ZitR_{IL}$ (5HYX, in magenta) or (B) $AdcR_{Spne}$ (3TGN, in blue) holo-dimers have been superimposed. Each protein is shown in ribbon representation with protomer A and B in dark and light color respectively, and labelled N and C-terminus. Zn(II) atoms are shown as spheres of the same color as the protein.
(TIF)

**S5 Fig. Structure conservation between ZitR proteins in the wHTH DNA-binding domain.** The structure of holo-$ZitR_{MG}$ (this study, 6FI9, in green) and that of either (A) WT DNA-bound $ZitR_{IL}$ (5YI2, in magenta) or (B) C30S DNA-bound $ZitR_{IL}$ (5YI3, in violet) holo-forms have been superimposed. Only a zoom on a small region of the wHTH DNA-binding domain of each protein (protomer A) is shown in ribbon representation. In the last two cases, DNA is in light color. Residues known to contact DNA in $ZitR_{IL}$ and the residues aligned to them in $ZitR_{MG}$ are represented as ball-and-sticks, in dark or light color depending on whether they are accessible or moderately accessible, with their N and O atoms colored in blue and red respectively, and labelled.
(TIF)

**S6 Fig. Sequence alignment between $ZitR_{MG}$ protein and other MarR superfamily members.** The sequence of $ZitR_{MG}$ (this study, 6FI9), and that of other MarR members (non-ZnRR proteins): RovA (4AIJ), SlyA (3Q5F), and OhrR (1Z9C) have been multi-aligned like in Fig 1. Secondary elements of $ZitR_{MG}$ protein are displayed above its sequence, and the accessibility of its residues is shown below the alignment using the following color code: dark blue, cyan and white respectively indicate fully accessible, moderately accessible and buried residues. Residues identical in all proteins are shown in white characters in a red background. Residues conserved in at least one, and up to three of the other MarR proteins are indicated as following: '3', '2' and '1' characters under the alignment respectively label residues conserved in all the three non-ZnRR MarR proteins (RovA, SlyA and OhR), in two of them (RovA and SlyA), or in only one of them OhrR.
(TIF)

**S7 Fig. Comparison of the Zn(II) binding sites between ZnRR proteins.** Zn(II) binding domains are compared between $ZitR_{MG}$ holo-dimer (in green) and either $ZitR_{IL}$ (in magenta, A-C) or $AdcR_{Spne}$ (in blue, D-F) holo-dimers (only protomer A is shown of each protein). The whole metal binding pocket (A, D), Zn(II) binding site 1 (B, E), and 2 (C, F) are represented. Zn(II) atoms are shown as spheres of the same color as the protein. Water molecules are represented as red spheres. Residues involved in Zn(II) binding are in ball-and-sticks with N, O and S atoms respectively colored in blue, red and yellow. Zn(II)-Zn(II) inter-nuclear distance is indicated close to a grey dashed line (A, D). In each comparison, only the residues of $ZitR_{IL}$ or $AdcR_{Spne}$ proteins are labelled.
(TIF)

## Acknowledgments

This work was supported by the French Infrastructure for Integrated Structural Biology (FRISBI), ANR-10-INSB-05-01. The structure data from this publication have been deposited in the PDB database https://www.rcsb.org/ and assigned the accession number 6FI9. This work has benefitted from the facilities and expertise of the IMAGIF Structural and Proteomic Biology Pole at the Research Center of Gif (https://www.imagif.cnrs.fr): crystallization, SICaPS, biophysics, CTPF and calorimetry (now I2BC); as well as the PROXIMA-1, PROXIMA-2A and DISCO beamlines at SOLEIL synchrotron (http://www.synchrotron-soleil.fr). We thank Herman Van Tilbeurgh (I2BC at Orsay), Nicolas Leulliot and Benjamin Dray (LCRB at Paris), for initial crystallization assays; Frank Wien (SOLEIL synchrotron) for SRCD experiments; Julie Ménétrey (I2BC at Gif) for discussion and Joni Frederick (I2BC at Gif) for English corrections.

## Author Contributions

**Conceptualization:** Paloma Fernández Varela, Isabelle Poquet.

**Data curation:** Paloma Fernández Varela, Christophe Velours, Magali Aumont-Niçaise, Pierre Legrand.

**Formal analysis:** Paloma Fernández Varela, Christophe Velours, Magali Aumont-Niçaise, Blandine Pineau, Pierre Legrand, Isabelle Poquet.

**Funding acquisition:** Paloma Fernández Varela.

**Investigation:** Paloma Fernández Varela, Christophe Velours, Magali Aumont-Niçaise, Pierre Legrand, Isabelle Poquet.

**Methodology:** Paloma Fernández Varela, Christophe Velours, Magali Aumont-Niçaise, Blandine Pineau, Pierre Legrand.

**Project administration:** Paloma Fernández Varela.

**Resources:** Paloma Fernández Varela.

**Software:** Paloma Fernández Varela, Pierre Legrand.

**Supervision:** Paloma Fernández Varela, Magali Aumont-Niçaise, Pierre Legrand.

**Validation:** Paloma Fernández Varela, Christophe Velours, Magali Aumont-Niçaise, Pierre Legrand, Isabelle Poquet.

**Visualization:** Paloma Fernández Varela, Christophe Velours, Blandine Pineau, Pierre Legrand.

**Writing – original draft:** Paloma Fernández Varela.

**Writing – review & editing:** Paloma Fernández Varela, Isabelle Poquet.

## References


1. Maret W. Zinc biochemistry: from a single zinc enzyme to a key element of life. Adv Nutr. 2013 Jan; 4(1):82–91. https://doi.org/10.3945/an.112.003038 PMID: 23319127
2. Tubek S, Grzanka P, Tubek I. Role of zinc in hemostasis: a review. Biol Trace Elem Res. 2008 Jan; 121(1):1–8. https://doi.org/10.1007/s12011-007-8038-y PMID: 17968515
3. Chandrangsu P, Rensing C, Helmann JD. Metal homeostasis and resistance in bacteria. Nat Rev Microbiol. 2017 Jun; 15(6):338–50. https://doi.org/10.1038/nrmicro.2017.15 PMID: 28344348
4. Capdevila DA, Wang J, Giedroc DP. Bacterial Strategies to Maintain Zinc Metallostasis at the Host-Pathogen Interface. J Biol Chem. 2016 Sep 30; 291(40):20858–68. https://doi.org/10.1074/jbc.R116.742023 PMID: 27462080
5. Lee JW, Helmann JD. Functional specialization within the Fur family of metalloregulators. Biometals. 2007 Jun; 20(3–4):485–99. https://doi.org/10.1007/s10534-006-9070-7 PMID: 17216355
6. Wilkinson SP, Grove A. Ligand-responsive transcriptional regulation by members of the MarR family of winged helix proteins. Curr Issues Mol Biol. 2006 Jan; 8(1):51–62. PMID: 16450885
7. Deochand DK, Grove A. MarR family transcription factors: dynamic variations on a common scaffold. Crit Rev Biochem Mol Biol. 2017 Dec; 52(6):595–613. https://doi.org/10.1080/10409238.2017.1344612 PMID: 28670937
8. Fillat MF. The FUR (ferric uptake regulator) superfamily: diversity and versatility of key transcriptional regulators. Arch Biochem Biophys. 2014 Mar 15; 546:41–52. https://doi.org/10.1016/j.abb.2014.01.029 PMID: 24513162
9. Perera IC, Grove A. Molecular mechanisms of ligand-mediated attenuation of DNA binding by MarR family transcriptional regulators. J Mol Cell Biol. 2010 Oct; 2(5):243–54. https://doi.org/10.1093/jmcb/mjq021 PMID: 20716550
10. Alekshun MN, Levy SB, Mealy TR, Seaton BA, Head JF. The crystal structure of MarR, a regulator of multiple antibiotic resistance, at 2.3 Å resolution. Nat Struct Biol. 2001 Aug; 8(8):710–4. https://doi.org/10.1038/90429 PMID: 11473263
11. Dintilhac A, Claverys JP. The *adc* locus, which affects competence for genetic transformation in *Streptococcus pneumoniae*, encodes an ABC transporter with a putative lipoprotein homologous to a family of streptococcal adhesins. Res Microbiol. 1997 Feb; 148(2):119–31. https://doi.org/10.1016/S0923-2508(97)87643-7 PMID: 9765793
12. Claverys JP. A new family of high-affinity ABC manganese and zinc permeases. Res Microbiol. 2001 Apr-May; 152(3–4):231–43. PMID: 11421271
13. Guerra AJ, Dann CE 3rd, Giedroc DP. Crystal structure of the zinc-dependent MarR family transcriptional regulator AdcR in the Zn(II)-bound state. J Am Chem Soc. 2011 Dec 14; 133(49):19614–7. https://doi.org/10.1021/ja2080532 PMID: 22085181
14. Shafeeq S, Kloosterman TG, Kuipers OP. Transcriptional response of *Streptococcus pneumoniae* to $Zn^{2+}$ limitation and the repressor/activator function of AdcR. Metallomics. 2011 Jun; 3(6):609–18. https://doi.org/10.1039/c1mt00030f PMID: 21603707

15. Llull D, Poquet I. New expression system tightly controlled by zinc availability in *Lactococcus lactis*. Appl Environ Microbiol. 2004 Sep; 70(9):5398–406. https://doi.org/10.1128/AEM.70.9.5398-5406.2004 PMID: 15345426

16. Llull D, Son O, Blanie S, Briffotaux J, Morello E, Rogniaux H, et al. *Lactococcus lactis* ZitR is a zinc-responsive repressor active in the presence of low, nontoxic zinc concentrations *in vivo*. J Bacteriol. 2011 Apr; 193(8):1919–29. https://doi.org/10.1128/JB.01109-10 PMID: 21317326

17. Dintilhac A, Alloing G, Granadel C, Claverys JP. Competence and virulence of *Streptococcus pneumoniae*: Adc and PsaA mutants exhibit a requirement for Zn and Mn resulting from inactivation of putative ABC metal permeases. Mol Microbiol. 1997 Aug; 25(4):727–39. PMID: 9379902

18. Reyes-Caballero H, Guerra AJ, Jacobsen FE, Kazmierczak KM, Cowart D, Koppolu UM, et al. The metalloregulatory zinc site in *Streptococcus pneumoniae* AdcR, a zinc-activated MarR family repressor. J Mol Biol. 2010 Oct 22; 403(2):197–216. https://doi.org/10.1016/j.jmb.2010.08.030 PMID: 20804771

19. Panina EM, Mironov AA, Gelfand MS. Comparative genomics of bacterial zinc regulons: enhanced ion transport, pathogenesis, and rearrangement of ribosomal proteins. Proc Natl Acad Sci U S A. 2003 Aug 19; 100(17):9912–7. https://doi.org/10.1073/pnas.1733691100 PMID: 12904577

20. Makthal N, Nguyen K, Do H, Gavagan M, Chandrangsu P, Helmann JD, et al. A Critical Role of Zinc Importer AdcABC in Group A *Streptococcus*-Host Interactions During Infection and Its Implications for Vaccine Development. EBioMedicine. 2017 Jul; 21:131–41. https://doi.org/10.1016/j.ebiom.2017.05.030 PMID: 28596134

21. Zhu R, Song Y, Liu H, Yang Y, Wang S, Yi C, et al. Allosteric histidine switch for regulation of intracellular zinc(II) fluctuation. Proc Natl Acad Sci U S A. 2017 Dec 26; 114(52):13661–6. https://doi.org/10.1073/pnas.1708563115 PMID: 29229866

22. Lees JG, Smith BR, Wien F, Miles AJ, Wallace BA. CDtool-an integrated software package for circular dichroism spectroscopic data processing, analysis, and archiving. Anal Biochem. 2004 Sep 15; 332(2):285–9. https://doi.org/10.1016/j.ab.2004.06.002 PMID: 15325297

23. Whitmore L, Wallace BA. Protein secondary structure analyses from circular dichroism spectroscopy: methods and reference databases. Biopolymers. 2008 May; 89(5):392–400. https://doi.org/10.1002/bip.20853 PMID: 17896349

24. Whitmore L, Wallace BA. DICHROWEB, an online server for protein secondary structure analyses from circular dichroism spectroscopic data. Nucleic Acids Res. 2004 Jul 1; 32(Web Server issue):W668–73. https://doi.org/10.1093/nar/gkh371 PMID: 15215473

25. Kabsch W. XDS. Acta Crystallogr D Biol Crystallogr. 2010 Feb; 66(Pt 2):125–32. https://doi.org/10.1107/S0907444909047337 PMID: 20124692

26. McCoy AJ, Grosse-Kunstleve RW, Adams PD, Winn MD, Storoni LC, Read RJ. Phaser crystallographic software. J Appl Crystallogr. 2007 Aug 1; 40(Pt 4):658–74. https://doi.org/10.1107/S0021889807021206 PMID: 19461840

27. Winn MD, Ballard CC, Cowtan KD, Dodson EJ, Emsley P, Evans PR, et al. Overview of the CCP4 suite and current developments. Acta Crystallogr D Biol Crystallogr. 2011 Apr; 67(Pt 4):235–42. https://doi.org/10.1107/S0907444910045749 PMID: 21460441

28. Blanc E, Roversi P, Vonrhein C, Flensburg C, Lea SM, Bricogne G. Refinement of severely incomplete structures with maximum likelihood in BUSTER-TNT. Acta Crystallogr D Biol Crystallogr. 2004 Dec; 60(Pt 12 Pt 1):2210–21. https://doi.org/10.1107/S0907444904016427 PMID: 15572774

29. Hong M, Fuangthong M, Helmann JD, Brennan RG. Structure of an OhrR-*ohrA* operator complex reveals the DNA binding mechanism of the MarR family. Mol Cell. 2005 Oct 7; 20(1):131–41. https://doi.org/10.1016/j.molcel.2005.09.013 PMID: 16209951

30. Robert X, Gouet P. Deciphering key features in protein structures with the new ENDscript server. Nucleic Acids Res. 2014 Jul; 42(Web Server issue):W320–4. https://doi.org/10.1093/nar/gku316 PMID: 24753421

31. Quade N, Mendonca C, Herbst K, Heroven AK, Ritter C, Heinz DW, et al. Structural basis for intrinsic thermosensing by the master virulence regulator RovA of *Yersinia*. J Biol Chem. 2012 Oct 19; 287(43):35796–803. https://doi.org/10.1074/jbc.M112.379156 PMID: 22936808

32. Dolan KT, Duguid EM, He C. Crystal structures of SlyA protein, a master virulence regulator of *Salmonella*, in free and DNA-bound states. J Biol Chem. 2011 Jun 24; 286(25):22178–85. https://doi.org/10.1074/jbc.M111.245258 PMID: 21550983

33. Lee JW, Soonsanga S, Helmann JD. A complex thiolate switch regulates the *Bacillus subtilis* organic peroxide sensor OhrR. Proc Natl Acad Sci U S A. 2007 May 22; 104(21):8743–8. https://doi.org/10.1073/pnas.0702081104 PMID: 17502599

34. Sanson M, Makthal N, Flores AR, Olsen RJ, Musser JM, Kumaraswami M. Adhesin competence repressor (AdcR) from *Streptococcus pyogenes* controls adaptive responses to zinc limitation and

contributes to virulence. Nucleic Acids Res. 2015 Jan; 43(1):418–32. https://doi.org/10.1093/nar/gku1304 PMID: 25510500

35. Saito K, Akama H, Yoshihara E, Nakae T. Mutations affecting DNA-binding activity of the MexR repressor of *mexR-mexA-mexB-oprM* operon expression. J Bacteriol. 2003 Oct; 185(20):6195–8. https://doi.org/10.1128/JB.185.20.6195-6198.2003 PMID: 14526032

36. Choi SH, Lee KL, Shin JH, Cho YB, Cha SS, Roe JH. Zinc-dependent regulation of zinc import and export genes by Zur. Nat Commun. 2017 Jun 9; 8:15812. https://doi.org/10.1038/ncomms15812 PMID: 28598435

37. Ma Z, Gabriel SE, Helmann JD. Sequential binding and sensing of Zn(II) by *Bacillus subtilis* Zur. Nucleic Acids Res. 2011 Nov; 39(21):9130–8. https://doi.org/10.1093/nar/gkr625 PMID: 21821657